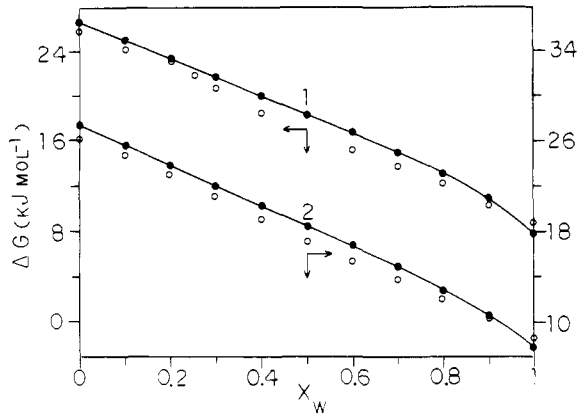

Figure 10. The free energy of hole formation $\overline{\Delta G_\sigma}$ and the free energy of activation of the viscosity ΔG_η^* as functions of the water mole fraction x_w, at 372 K: (1) $AgNO_3$-$TlNO_3$-$Cd(NO_3)_2$-H_2O and (2) $AgNO_3$-$TlNO_3$-$Ca(NO_3)_2$-H_2O; (●) ΔG_η^* and (○) $\overline{\Delta G_\sigma}$.

of activation of viscous flow, V is the molar volume, R is the gas constant, and h is the Planck constant.

For the salt-water systems of this study, over the whole concentration range, average values of ΔG_σ were calculated taking into account all the species in the solutions:

$$\overline{\Delta G_\sigma} = 4\pi\sigma N_A \overline{r_i^2} \tag{18}$$

The parameter $\overline{r_i^2}$ is the weight average of the squared particle radii given by

$$\overline{r_i^2} = \frac{x_s[\sum_i X_i(r_{i+}^2 + z_{i+}r_-^2)] + x_w r_w^2}{x_s[\sum_i X_i(1 + z_{i+})] + x_w} \tag{19}$$

The values of $\overline{\Delta G_\sigma}$ obtained from eq 18 and those of ΔG_η^* in eq 17 determined in previous investigations,[13,15] for the nitrate-water systems at 372 K, are plotted against x_w in Figures 9 and 10. It can be seen that $\overline{\Delta G_\sigma}$ is close to ΔG_η^*. These results lend support to the assumption that hole formation is an essential step of the viscous flow mechanisms not only in certain types of molten salts but in dilute aqueous solutions and water as well, above ordinary temperatures.

Contrary to $\overline{\Delta G_\sigma}$ and ΔG_η^*, the entropy of hole formation and that of activation in viscous flow cannot be compared to one another, since the particle radii provide approximate evaluations of hole sizes and their variation with the temperature is not known.

4. Conclusion

This study showed that the application of the Guggenheim and Adam method and the Butler equation yield reasonable orders of magnitude of the water mole fraction, activity, and activity coefficient in the surface phase of some nitrate-water melts, over the whole concentration range from fused salts to water. The correlation between the water activity, or activity coefficient, in the surface phase and the hydrating power of the cations predispose to consider the monolayer surface phase as a convenient model. Besides, it was found that the free energy of hole formation in the Fürth theory of liquids is close to the free energy of activation for the viscous flow in the Eyring equation. This result tends to confirm that holes may be considered as fundamental structural entities in the chemistry of all solutions from molten salts to water.

Sequential Bond Energies of $Fe(CO)_x^+$ (x = 1-5): Systematic Effects on Collision-Induced Dissociation Measurements

Richard H. Schultz, Kevin C. Crellin, and P. B. Armentrout*,†

Contribution from the Department of Chemistry, University of Utah, Salt Lake City, Utah 84112.
Received May 16, 1991

Abstract: Collision-induced dissociation (CID) of $Fe(CO)_x^+$ (x = 1-5) is studied by using guided ion beam mass spectrometry. A flow tube source is used to produce thermalized iron carbonyl ions. We discuss in detail our threshold modeling procedures and several possible sources of systematic error that can affect accurate determination of bond energies from CID threshold measurements. Careful analysis of CID thresholds provides the following 0 K bond dissociation energies: $D°[(CO)_4Fe^+-CO]$ = 1.16 ± 0.04 eV (26.8 ± 0.9 kcal/mol); $D°[(CO)_3Fe^+-CO]$ = 1.07 ± 0.07 eV (24.7 ± 1.4 kcal/mol); $D°[(CO)_2Fe^+-CO]$ = 0.69 ± 0.05 eV (15.9 ± 1.2 kcal/mol); and $D°[(CO)Fe^+-CO]$ = 1.61 ± 0.15 eV (36.1 ± 1.8 kcal/mol). We also measure $D°[Fe^+-CO]$ = 1.59 ± 0.08 eV (36.6 ± 1.8 kcal/mol), but this dissociation may correspond to production of excited $Fe^+(^4F)$, in which case the $D°[Fe^+-CO]$ for dissociation to $Fe^+(^6D)$ is 1.36 ± 0.08 eV (31.3 ± 1.8 kcal/mol). The sum of the five bond energies, 6.12 ± 0.09 eV (140.1 ± 3.1 kcal/mol), is in excellent agreement with literature thermochemistry, and the individual bond strengths are in reasonable accord with prior measurements and theoretical calculations.

Introduction

In the century since the first synthesis of $Fe(CO)_5$,[1] iron carbonyl and its derivatives have found myriad uses as reagents for chemical synthesis.[2] Besides numerous reactivity studies, a considerable amount of experimental[3-7] and theoretical[8-11] effort has gone into elucidating the fundamental physical properties of these species. A similarly large research effort has been devoted to iron carbonyl ions. While these ions (especially the anions) are known and have been studied in solution,[12] most of the work concerning them has been done in the gas phase. The gas phase is an ideal arena for detailed study of these highly reactive species. Solvation effects are absent, and the coordinatively and electronically unsaturated ions can be isolated and their reactivity observed.

† Camille and Henry Dreyfus Teacher-Scholar, 1987-1992.

(1) Mond, L.; Quincke, F. *J. Chem. Soc.* **1891**, *59*, 604. Mond, L.; Langler, C. *J. Chem. Soc.* **1891**, *59*, 1090. Berthelot, M. *C. R. Acad. Sci.* **1891**, *112*, 1343.

(2) Examples of the many applications of iron carbonyl species can be found in (a) Alper, H. In *Organic Synthesis via Metal Carbonyls*; Wender, I., Pino, P., Eds.; Wiley-Interscience: New York, 1977; Vol. 2, p 545. (b) Poliakoff, M. *Chem. Soc. Rev.* **1978**, *7*, 527. (c) Collman, J. P.; Hegedus, L. S. *Principles and Applications of Organotransition Metal Chemistry*; University Science Books: Mill Valley, CA, 1980. (d) Bailey, D. C.; Langer, S. H. *Chem. Rev.* **1981**, *81*, 109. (e) Davies, S. G. *Organotransition Metal Chemistry: Applications to Organic Synthesis*; Pergamon: New York, 1982. (f) Brunet, J.-J. *Chem. Rev.* **1990**, *90*, 1041.

(3) Jones, L. H.; McDowell, R. S.; Goldblatt, M.; Swanson, B. I. *J. Chem. Phys.* **1972**, *57*, 2050.

0002-7863/91/1513-8590$02.50/0

Table I. Summary of Values for $D°[(CO)_xFe^+-CO]$ (kcal/mol)

bond	Distefano[a]	NAFN[b]	this study
Fe^+-CO	57.6 ± 2.3	39.3 ± 2.0	36.6 ± 1.8
	[36.9],[c] (31.6)[c,d]	(34.0 ± 2.0)[d]	(31.3 ± 1.8)[d]
$COFe^+-CO$	19.6 ± 2.3	41.5 ± 1.6	36.1 ± 1.2
	[40.3][c]		
$(CO)_2Fe^+-CO$	18.7 ± 2.3	25.7 ± 1.4	15.9 ± 1.4
$(CO)_3Fe^+-CO$	25.4 ± 2.3	25.2 ± 1.1	24.7 ± 1.4
$(CO)_4Fe^+-CO$	18.2 ± 2.3	17.8 ± 0.9	26.8 ± 0.9
sum of BDEs[e]	139.5 ± 5.2	149.5 ± 3.2[f]	140.0 ± 3.1
	(134.2 ± 5.2)[d]	(144.2 ± 3.2)[d]	(134.8 ± 3.1)[d]

[a] Reference 17. [b] Reference 23. [c] Value adjusted as in ref 19; see text. [d] Numbers in parentheses are corrected for the possibility that the observed dissociation of $FeCO^+$ is to the diabatic $Fe^+(^4F)$ state; see text. [e] Literature sum of BDEs (Table II) is 136.4 ± 1.9 kcal/mol at 0 K; see text. [f] This value is the sum of the individual BDEs determined by PEPICO. The value of $\Delta_f H°(1)$ given in the text, 149.9 ± 1.6 kcal/mol, is that reported by NAFN, who derived it from the difference in the Fe^+ and $Fe(CO)_5^+$ appearance energies as measured by PI.

Table II. Literature Thermochemistry Used in This Paper[a]

species	$\Delta_f H°$(0 K), kcal/mol	$\Delta_f H°$(298 K), kcal/mol
C_2H_6		−20.1 ± 0.05[b]
$(CH_3)_2CO$		−51.9 ± 0.1[b]
CO	−27.20 ± 0.04	−26.42 ± 0.04
Fe	98.73 ± 0.06	99.31 ± 0.06
Fe^+	280.96 ± 0.06[c]	283.026 ± 0.06[c,d]
$Fe(CO)_5$(g)	−173.96 ± 1.70	−174.36 ± 1.70
$Fe(CO)_5^+$	8.91 ± 1.84[e]	9.99 ± 1.84[d,e]

[a] Unless otherwise stated, all data in this table are taken from ref 45. [b] Reference 47. [c] IE(Fe) = 7.9024 ± 0.0001 eV (182.234 ± 0.002 kcal/mol), taken from ref 50. [d] Includes 1.48 kcal/mol for the enthalpy of the electron (thermal electron convention). [e] Using IE[$Fe(CO)_5$] = 7.93 ± 0.03 eV; see text.

$Fe(CO)_x^+$ ions have been the subject of many investigations[13] directed at determining the sequential $(CO)_xFe^+-CO$ bond dissociation energies (BDEs). Theorists have calculated that the bonding between metal ions and CO is primarily electrostatic for $x = 0$ and 1, with minimal back-bonding.[14] One theoretical study that did calculations specifically on the bonding in $FeCO^+$ and $Fe(CO)_2^+$ predicts[11] a quartet ground state for both ions and D_es of 30.3 and 34.5 kcal/mol, respectively. There have been numerous experimental attempts to obtain these BDEs as well. Several photoionization[15-17] (PI) and electron impact (EI) appearance potential[18] studies have attempted to measure the individual bond strengths by measuring relative appearance energies for the various $Fe(CO)_x^+$ ions from neutral $Fe(CO)_5$ and taking the differences to be the bond strengths. These studies are likely to give an accurate value for the ionization energy (IE) of the neutral, but are less likely to be accurate for the individual bond strengths, since the difficulty of accurately measuring the appearance energy increases as more carbonyls are removed. Indeed, Halle et al.[19] have suggested that the Distefano's original PI data[17] support a value of 36.9 kcal/mol for the BDE of Fe^+-CO rather than the originally reported BDE of 57.6 kcal/mol.

Another approach to finding individual BDEs is to measure photodissociation thresholds for individual $Fe(CO)_x^+$ ions rather than ionization thresholds for neutral species. Cassady and Freiser[20] used such a technique to obtain an upper limit of 43 ± 3 kcal/mol to the Fe^+-CO bond strength. Tecklenberg et al.[21] attempted to derive such BDEs from photodissociation of $Fe(CO)_x^+$ ions for $x = 1-5$. The only $Fe(CO)_x^+$ ion that photodissociated over the wavelength range of 458-514.5 nm (2.71-2.41 eV) was $Fe(CO)_4^+$, implying that the $Fe(CO)_x^+$ ions are unusually strongly bound, that their photodissociation cross sections in this wavelength range are low, or that photodissociation occurs too slowly to be observed in their experiment. From UV photodissociation of $Fe(CO)_5^+$, they were able to provide an upper limit of ~1.1 eV (25 kcal/mol) for the *average* $(CO)_{x-1}Fe^+-CO$ BDEs for $x = 3-5$ and 1.7 eV (39 kcal/mol) for $x = 1$ and 2.

Another determination of $D°(Fe^+-CO)$ was made via an entirely different technique by van Koppen et al.[22] They measured the kinetic energy release distributions of $FeCO^+$ formed by decomposition of the Fe^+/acetone complex. From this study, they obtained a 0 K value of 26 ± 5 kcal/mol for the Fe^+-CO bond strength.

The most recent experimental attempt to determine the $(CO)_xFe^+-CO$ BDEs is a photoelectron-photoion coincidence (PEPICO) and photoionization study by Ng and co-workers (NAFN).[23] This study reported more precise values for the bond strengths than previous PI and EI experiments, Table I. The studies of van Koppen et al. and of NAFN and their relationship to the present one are discussed in more detail below.

Reactions of $Fe(CO)_x^+$ ions have been investigated as well. Foster and Beauchamp[24] performed an ICR experiment on various iron carbonyl ions. They observed both clustering reactions of $Fe(CO)_x^+$ ions with $Fe(CO)_5$ and ligand displacement reactions of a number of molecules with $Fe(CO)_x^+$ ions. Their observation of displacement of CO molecules by H_2O molecules is inconclusive, however, for determining relative thermochemistry. Since Foster and Beauchamp produced the ions for their study by electron impact on $Fe(CO)_5$, their experiment may be complicated by an unknown amount of reactivity by excited ions. Freas and Ridge[25]

(4) Peden, C. H. F.; Parker, S. F.; Barrett, P. H.; Preason, R. G. *J. Phys. Chem.* **1983**, *87*, 2329. De Paoli, M. A.; de Oliveira, S. M.; Baggio-Saitovitch, E.; Guenzberger, D. *J. Chem. Phys.* **1984**, *80*, 730. Bominaar, E.; Guillin, J.; Marathe, V. R.; Sawaryn, A.; Trautwein, A. X. *Hyperfine Interact.* **1988**, *40*, 111.
(5) Lionel, T.; Morton, J. R.; Preston, K. F. *J. Chem. Phys.* **1982**, *76*, 234.
(6) Green, J. C.; Jackson, S. E. *J. Chem. Soc., Dalton Trans.* **1976**, 1698. Poliakoff, M.; Ceulemans, A. *J. Am. Chem. Soc.* **1984**, *106*, 50. Miller, M. E.; Grant, E. R. *J. Am. Chem. Soc.* **1985**, *107*, 3386. Nagano, Y.; Achiba, Y.; Kimura, K. *J. Phys. Chem.* **1986**, *90*, 1288. Weiller, B. H.; Grant, E. R. *J. Am. Chem. Soc.* **1987**, *109*, 1051. Smith, G. P. *Polyhedron* **1988**, *7*, 1605.
(7) Ouderkirk, A. J.; Weitz, E. *J. Chem. Phys.* **1983**, *79*, 1089. Ouderkirk, A. J.; Wermer, P.; Schultz, N. L.; Weitz, E. *J. Am. Chem. Soc.* **1983**, *105*, 3354. Poliakoff, M.; Weitz, E. *Acc. Chem. Res.* **1987**, *20*, 408. Weitz, E. *J. Phys. Chem.* **1987**, *91*, 3945. Seder, T. A.; Ouderkirk, A. J.; Weitz, E. *J. Chem. Phys.* **1986**, *85*, 1977.
(8) Hoskins, B. R.; Whillans, F. D. *Coord. Chem. Rev.* **1973**, *9*, 365. Rossi, A. R.; Hoffman, R. *Inorg. Chem.* **1975**, *14*, 365.
(9) Guenzburger, D.; Saitovitch, E. M. B.; De Paoli, M. A.; Manela, H. *J. Chem. Phys.* **1984**, *80*, 735. Daniel, C.; Bénard, M.; Dedieu, A.; Wiest, R.; Veillard, A. *J. Phys. Chem.* **1984**, *88*, 4805. Guerra, M.; Jones, D.; Distefano, G.; Foffani, A.; Modelli, A. *J. Am. Chem. Soc.* **1988**, *110*, 375.
(10) Bauschlicher, C. W., Jr.; Bagus, P. S. *J. Chem. Phys.* **1984**, *81*, 5889. Bauschlicher, C. W., Jr.; Bagus, P. S.; Nelin, C. J.; Roos, B. O. *J. Chem. Phys.* **1986**, *85*, 354. Barnes, L. A.; Rosi, M.; Bauschlicher, C. W., Jr. *J. Chem. Phys.* **1990**, *94*, 2031.
(11) Barnes, L. A.; Rosi, M.; Bauschlicher, C. W., Jr. *J. Chem. Phys.* **1990**, *93*, 609.
(12) See, for example: Krusic, P. J.; San Fillipo, J., Jr.; Hutchison, B.; Hance, R. L.; Daniels, L. M. *J. Am. Chem. Soc.* **1981**, *103*, 2129. Theirien, M. J.; Trogler, W. C. *J. Am. Chem. Soc.* **1986**, *108*, 3697.
(13) While this report concerns cationic species, $Fe(CO)_x^-$ ions have received considerable gas-phase study as well. Representative references include Compton, N.; Stockdale, J. A. D. *Int. J. Mass Spectrom. Ion Phys.* **1976**, *22*, 47. Engelking, P. C.; Lineberger, W. C. *J. Am. Chem. Soc.* **1979**, *101*, 5569. McDonald, R. N.; Chowdhury, A. K.; Jones, M. T. *J. Am. Chem. Soc.* **1986**, *108*, 3105. Lane, K. R.; Squires, R. R. *Polyhedron* **1988**, *7*, 1609.
(14) Barnes, L. A.; Bauschlicher, Jr., C. W. *Chem. Phys.* **1988**, *124*, 383. Mavridis, A.; Harrison, J. F.; Allison, J. *J. Am. Chem. Soc.* **1989**, *111*, 2482.
(15) Vilesov, F. I.; Kurbatov, B. L. *Proc. Acad. Sci. USSR, Phys. Chem. Sect.* **1961**, *140*, 792.
(16) Lloyd, D. R.; Schlag, E. W. *Inorg. Chem.* **1969**, *8*, 2544.
(17) Distefano, G. *J. Res. Natl. Bur. Stand., Sect. A* **1970**, *74*, 233.
(18) Winters, R. E.; Kiser, R. W. *Inorg. Chem.* **1964**, *3*, 699. Foffani, A.; Pignataro, S.; Cantone, B.; Grasso, F. *Z. Phys. Chem. (Frankfurt/Main)* **1965**, *45*, 79. Bidinosti, D. R.; McIntyre, N. S. *Can. J. Chem.* **1967**, *45*, 641. Junk, G. A.; Svec, H. J. *Z. Naturforsch.* **1968**, *23b*, 1.
(19) Halle, L. F.; Armentrout, P. B.; Beauchamp, J. L. *Organometallics* **1982**, *1*, 963.
(20) Cassady, C. J.; Freiser, B. S. *J. Am. Chem. Soc.* **1984**, *106*, 6176.
(21) Tecklenberg, R. E., Jr.; Bricker, D. L.; Russell, D. H. *Organometallics* **1988**, *7*, 2506.
(22) van Koppen, P. A. M.; Jacobson, D. B.; Illies, A.; Bowers, M. T.; Hanratty, M.; Beauchamp, J. L. *J. Am. Chem. Soc.* **1989**, *111*, 1991.
(23) Norwood, K.; Ali, A.; Flesch, G. D.; Ng, C. Y. *J. Am. Chem. Soc.* **1990**, *112*, 7502.
(24) Foster, M. S.; Beauchamp, J. L. *J. Am. Chem. Soc.* **1975**, *97*, 4808.
(25) Freas, R. B.; Ridge, D. P. *J. Am. Chem. Soc.* **1980**, *102*, 7129.

used ICR to observe the thermal energy reactions of Fe^+ and $FeCO^+$ formed by electron impact on $Fe(CO)_5$ with n-C_4D_{10} and i-C_4D_{10}. They found that while the atomic ion reacts with butanes to eliminate hydrogen or an alkane, $FeCO^+$ only undergoes substitution of the CO ligand by the butane reactant. Ridge and co-workers used this substitution technique to form Fe^+/alkane[26] and Fe^+/alkene[27] complexes for further study. One reaction study provides information on the Fe^+–CO BDE. Using ion cyclotron resonance (ICR), Freiser and co-workers[28] observed that Fe^+ can exothermically eliminate ethane from acetone, thus implying that Fe^+–CO > 5.4 ± 0.1 kcal/mol, Table II.

The present study was undertaken primarily to provide accurate values for the $(CO)_xFe^+$–CO BDEs and to resolve some of the discrepancies in the literature. To this end, we use low-energy collision-induced dissociation (CID). CID has been used to determine thermochemical and structural information about polyatomic ions,[29,30] ligated transition-metal ions,[31-35] and atomic cluster ions.[36-39] The advantage of this technique is that the CID threshold should provide a direct determination of the bond strength if the internal energy of the ion of interest is known.

We also undertook this work as a model study for the proper analysis of threshold excitation functions for CID processes. The $Fe(CO)_x^+$ system should provide a good test for the presence of systematic errors since the sum of the bond strengths measured here must agree with $\Delta_f H°(1)$, the enthalpy for complete fragmentation of $Fe(CO)_5^+$, reaction 1. This check on our final thermochemistry can also aid us in determining which threshold modeling procedures (if any) can give reliable thermochemistry from the experimentally observed CID excitation functions.

$$Fe(CO)_5^+ \rightarrow Fe^+ + 5CO \qquad (1)$$

Literature Thermochemistry

An accurate determination of the value of the enthalpy of reaction for reaction 1 depends on an accurate knowledge of $\Delta_f H°$ for Fe, CO, and $Fe(CO)_5$ and the IEs of Fe and $Fe(CO)_5$. The thermochemistry of Fe, Fe^+, and CO is well established, Table II. The values of $\Delta_f H°[Fe(CO)_5(g)]$ reported in the literature all ultimately derive from the combustion calorimetry data of Mittasch,[40] who reported $\Delta_f H°[Fe(CO)_5(l)] = -187.8$ kcal/mol, or Cotton et al.,[41] who reported $\Delta_f H°[Fe(CO)_5(l)] = -182.6$ kcal/mol. Wagman et al.[42] in the NBS tables and Behrens[43] cite a value of −185.0 kcal/mol, presumably an average of these two values. Pilcher and Skinner[44] and the JANAF tables[45] use only the value determined by Cotton et al. and discount the value of Mittasch due to less accurate characterization of the iron oxide products. The JANAF tables use the value of Cotton et al. for the heat of combustion of $Fe(CO)_5$ combined with their own values for the heats of formation of Fe_2O_3 and CO_2 to derive $\Delta_f H°[Fe(CO)_5(l)] = -183.10 \pm 1.70$ kcal/mol at 298.15 K.

To obtain the gas-phase heat of formation of $Fe(CO)_5$, we need to add the heat of vaporization at 298.15 K to the heat of formation of the liquid. Unfortunately, there are several values in the literature for this quantity as well. Cotton et al.[41] cite a 1952 value for $\Delta_{vap}H°[Fe(CO)_5]$ of 8.9 kcal/mol[46] to yield a gas-phase heat of formation for $Fe(CO)_5$ of −173.7 ± 1.7 kcal/mol. Pilcher and Skinner[44] obtain $\Delta_f H°[Fe(CO)_5(g)]$ of −173.3 ± 1.6 kcal/mol by using an unreferenced value of 9.6 ± 0.2 kcal/mol for $\Delta_{vap}H°[Fe(CO)_5]$; this value for $\Delta_f H°[Fe(CO)_5(g)]$ is cited by Lias et al.[47] in their thermochemistry compilation. Behrens[43] and JANAF tables[45] use essentially the same set of experimental values[48] to derive different values for $\Delta_{vap}H°[Fe(CO)_5]$ of 9.84 and 9.14 kcal/mol, respectively, yielding respective values for $\Delta_f H°[Fe(CO)_5(g)]$ of −175.2 ± 3.0 and −174.0 ± 1.7 kcal/mol. The thermochemistry adopted in this paper, Table II, is taken from the JANAF tables because they provide a consistent and critically reviewed set of thermochemical data. For purposes of comparison, we note that NAFN[23] use the value recommended by Behrens.[43] We also note that if we use the *average* of the literature values for $\Delta_{vap}H°[Fe(CO)_5]$ and $\Delta_f H°[Fe(CO)_5(l)]$, then we obtain $\Delta_f H°[Fe(CO)_5(g)] = -176.1 \pm 3.3$ kcal/mol, which is within the experimental error of the value used in the JANAF tables.

A further complication that can arise in thermodynamic calculations is the conversion of $\Delta_f H°$ values from 298 to 0 K. Both Behrens and the JANAF tables cite a value of 7.92 kcal/mol for $H°(0\ K) - H°(298\ K)$ for $Fe(CO)_5$, i.e., the enthalpy difference between 298 and 0 K. To convert the heat of formation from one temperature to the other, we also need to take into account the 0–298 K enthalpy differences for the elements in their standard states, Fe, C (graphite), and O_2 (1.077, 0.251, and 2.075 kcal/mol, respectively[45]). The difference in the 298 and 0 K heats of formation for $Fe(CO)_5$ is thus only 0.40 kcal/mol, such that $\Delta_f H°_0[Fe(CO)_5]$ is −174.4 ± 1.7 kcal/mol,[45] Table II (−176.5 ± 3.3 kcal/mol if the average literature thermochemistry is used).

The final thermochemical value needed to determine $\Delta_f H°(1)$ is the IE of $Fe(CO)_5$. Once again, there are a number of values available in the literature from which to choose. Three PI experiments obtain values of 7.95 ± 0.03,[15] 7.96 ± 0.02,[16] and 7.98 ± 0.01 eV,[17] respectively. More recently, NAFN obtained values for the IE of 7.877 ± 0.020 eV by PI and of 7.897 ± 0.025 eV by PEPICO. For purposes of the present discussion, we adopt the average of all five values, 7.933 ± 0.044 eV, as IE[$Fe(CO)_5$], Table II.

From the literature thermochemistry in Table II, we derive a value for $\Delta_f H°(1)$ of 136.4 ± 1.9 kcal/mol at 0 K, or 140.5 kcal/mol at 298 K. NAFN measured a value for $\Delta_f H°(1)$ as the difference in the photoionization appearance energies for $Fe(CO)_5^+$ (7.877 ± 0.02 eV) and Fe^+ (14.38 ± 0.07 eV). Since they pro-

(26) Larsen, B. S.; Ridge, D. P. *J. Am. Chem. Soc.* **1984**, *106*, 1912.
(27) Peake, D. A.; Gross, M. L.; Ridge, D. P. *J. Am. Chem. Soc.* **1984**, *106*, 4307.
(28) Burnier, R. C.; Byrd, G. D.; Freiser, B. S. *J. Am. Chem. Soc.* **1981**, *103*, 4360.
(29) Aristov, N.; Armentrout, P. B. *J. Phys. Chem.* **1986**, *90*, 5135.
(30) Schultz, R. H.; Armentrout, P. B. *Int. J. Mass Spectrom. Ion Processes* **1991**, *107*, 29.
(31) Magnera, T. F.; David, D. E.; Michl, J. *J. Am. Chem. Soc.* **1989**, *111*, 4100.
(32) Marinelli, P. J.; Squires, R. R. *J. Am. Chem. Soc.* **1989**, *111*, 4101.
(33) Jacobson, D. B.; Freiser, B. S. *J. Am. Chem. Soc.* **1983**, *105*, 736.
(34) Magnera, T. F.; David, D. E.; Stulik, D.; Orth, R. G.; Jonkman, H. T.; Michl, J. *J. Am. Chem. Soc.* **1989**, *111*, 5036.
(35) We have performed other studies of CID in FeL_x^+ systems: (a) Schultz, R. H.; Armentrout, P. B. *J. Phys. Chem.*, submitted for publication. (b) Schultz, R. H.; Armentrout, P. B. *J. Am. Chem. Soc.*, submitted for publication. (c) Schultz, R. H.; Armentrout, P. B. *Organometallics*, submitted for publication.
(36) Hanley, L.; Anderson, S. L. *J. Phys. Chem.* **1987**, *91*, 5161.
(37) Jarrold, M. F.; Bower, J. E. *J. Phys. Chem.* **1988**, *92*, 5702.
(38) Loh, S. K.; Lian, L.; Hales, D. A.; Armentrout, P. B. *J. Chem. Phys.* **1988**, *89*, 3378.
(39) Loh, S. K.; Hales, D. A.; Lian, L.; Armentrout, P. B. *J. Chem. Phys.* **1989**, *90*, 5466. Hales, D. A.; Lian, L.; Armentrout, P. B. *Int. J. Mass Spectrom. Ion Processes* **1990**, *102*, 269.
(40) Mittasch, A. *Angew. Chem.* **1928**, *41*, 827.
(41) Cotton, F. A.; Fischer, A. K.; Wilkinson, G. *J. Am. Chem. Soc.* **1959**, *81*, 800.
(42) Wagman, D. D.; Evans, W. H.; Parker, V. B.; Schumm, R. H.; Halow, I.; Bailey, S. M.; Churney, K. L.; Nuttall, R. L. *J. Phys. Chem. Ref. Data, Suppl. No. 2* **1982**, *11*, 1.
(43) Behrens, R. G. *J. Less-Common Met.* **1977**, *56*, 55.
(44) Pilcher, G.; Skinner, H. A. In *The Chemistry of the Metal-Carbon Bond*; Hartley, F. R., Patai, S., Eds.; Wiley: New York, 1982; Vol. 1 Chapter 2.
(45) Chase, M. W., Jr.; Davies, C. A.; Downey, J. R., Jr.; Frurip, D. J.; McDonald, R. A.; Syverud, A. N. *J. Phys. Chem. Ref. Data, Suppl. No. 1* **1985**, *14*, 1.
(46) *Selected Values of Chemical Thermodynamic Properties*; U.S. National Bureau of Standards Circular 500; U.S. Government Printing Office: Washington, DC, 1952.
(47) Lias, S. G.; Bartmess, J. E.; Liebman, J. F.; Homes, J. L.; Levin, R. D.; Mallard, W. G. *J. Phys. Chem. Ref. Data, Suppl. No. 1* **1988**, *17*, 1.
(48) Dewar, J.; Jones, H. O. *Proc. R. Soc. London* **1905**, *76*, 558. Eyber, G. *Z. Phys. Chem., Abt. A* **1929**, *144*, 1. Trautz, M.; Badstubner, W. *Z. Elektrochem.* **1929**, *35*, 799. Leadbetter, A. J.; Spice, J. E. *Can. J. Chem.* **1959**, *37*, 1923. Gilbert, A. G.; Sulzmann, K. G. P. *J. Electrochem. Soc.* **1974**, *121*, 832. The JANAF Tables also cite Baev, A. K. *Obshch. Prikl. Khim.* **1970**, *2*, 146.

duced their ions in a supersonic expansion, they assumed that their thresholds were typical of 0 K thermochemistry. Their $\Delta_f H°(1)$ of 6.50 ± 0.07 eV (149.9 ± 1.6 kcal/mol) is significantly larger than that calculated above for either 0 or 298 K. NAFN did not comment on this discrepancy because they incorrectly converted their results to a 298 K value of $\Delta_f H°[Fe(CO)_5(g)]$ that is within experimental error of the literature value.[49] There are several possible sources for the discrepancy. One is that dissociation yields the ^4F first excited state of Fe^+, to which $FeCO^+$ is expected to dissociate asymptotically.[11] NAFN did conclude that this dissociation pathway is operative, but even so, it can only account for 5.35 kcal/mol of the discrepancy at 0 K, that being the energy difference[50] between the ground $^6D_{9/2}$ and first excited $^4F_{9/2}$ states of Fe^+. Another possibility is that the literature value for the heat of formation of $Fe(CO)_5$ is incorrect. Working backward from their $\Delta_f H°(1)$, one obtains a value for $\Delta_f H°[Fe(CO)_5(g)]$ at 0 K of −188.0 ± 1.7 kcal/mol, or −186.9 kcal/mol if their value for the IE is used. None of the literature cited above, however, carries any hint that the literature thermochemistry for $Fe(CO)_5$ could be inaccurate by so much. The most likely explanation for the difference between the total obtained by NAFN and the literature is that the measured appearance energy for Fe^+ in the PI experiment is high due to a kinetic shift. The loss of all five ligands from photoionized $Fe(CO)_5^+$ is improbable at its threshold, such that the true thermodynamic threshold is difficult to observe. In their related CID experiment, NAFN measured a lower Fe^+–CO bond strength than from the PI experiment, possibly indicating a kinetic shift in the latter's threshold. Even using their CID value for $D°(Fe^+–CO)$ is not enough to account for the discrepancy between the sum of the BDEs they report and the literature thermochemistry discussed above, however. Similar difficulties may also affect Distefano's PI experiment,[17] although his value for $\Delta_f H°(1)$, 6.05 ± 0.1 eV (139.5 ± 2.3 kcal/mol), is in agreement with the literature value.

From this examination of the literature thermochemistry, we conclude that the possibility of the literature thermochemistry being widely in error is small. All discrepancies between prior measurements of $\Delta_f H°(1)$ and that calculated from the literature can be explained. Consequently, comparing our value for $\Delta_f H°(1)$ to that from the literature is likely to be a good test of whether we have measured the bond strengths accurately.

Experimental Section

The guided ion beam instrument on which these experiments were performed has been described in detail previously.[30,51] Ions are created in a flow tube source, described below, extracted from the source, accelerated, and passed through a magnetic sector for mass analysis. The mass-selected ions are then decelerated to the desired kinetic energy and focused into an octopole ion beam guide. This device uses radio frequency electric fields to trap the ions in the radial direction and ensure complete collection of reactant and product ions. The octopole passes through a gas cell of effective length 8.6 cm that contains the neutral collision partner (in these experiments, Xe or Ar) at a pressure sufficiently low that multiple ion–molecule collisions are improbable. The unreacted parent and product ions drift to the end of the octopole from which they are extracted, passed through a quadrupole mass filter for mass analysis, and detected using standard pulse counting techniques. Raw ion intensities are converted to cross sections as described previously.[51] We estimate absolute cross sections to be accurate to ±20%, while relative cross sections are accurate to ±5%.

Laboratory (lab) energies are converted to center of mass (CM) energies by using the conversion $E_{CM} = E_{lab}M/(M + m)$, where m and M are the ion and neutral masses, respectively. The absolute energy scale and corresponding full width at half-maximum (fwhm) of the ion beam kinetic energy distribution are determined by using the octopole as a retarding energy analyzer as described previously.[51] The absolute uncertainty in the energy scale is ±0.05 eV (lab). The energy distributions are nearly Gaussian and have typical fwhms of 0.25–0.4 eV (lab).

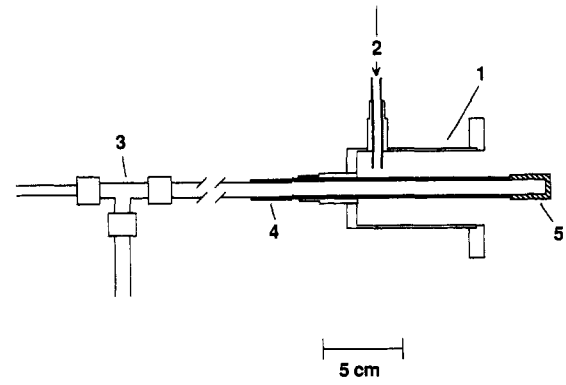

Figure 1. Schematic of the cold cathode dc discharge source: 1, source flange and can; 2, He and Ar inlet; 3, water cooling tube; 4, Pyrex insulating tube; 5, metal cathode cap.

Ion Sources. $Fe(CO)_x^+$ ions are produced in a flow tube ion source, described in detail elsewhere.[30] A fast flow of He gas (typically ~7500 standard cm^3/min) passes through a liquid N_2 trap to remove condensible impurities and then between the filament and extraction plate of an electron impact source at the end of a 1-m-long, 5-cm-diameter flow tube. Typical electron energies are 30–70 eV. $Fe(CO)_5$ is admitted to the tube several centimeters downstream and ionized and fragmented by charge transfer from He^+ or Penning ionization from He^*. At typical flow tube pressures of 0.5–0.6 Torr, the ions will undergo on the order of 10^5 thermalizing collisions as they traverse the flow tube. Ions are extracted from the flow tube and gently focused through a 9.5-cm-long differentially pumped region before entering the rest of the instrument described above. Lineberger and co-workers[52] have used photoelectron spectroscopy to determine that their flow tube (similar in design to ours) produces negative ions rotationally cooled to 300 K and vibrationally cooled to 300–1000 K. We expect that the ions studied here should be cooled easily, as they have low-frequency vibrational modes and can undergo ligand exchange with CO dissociated from other molecules. We therefore assume that the ions studied here are cooled to 300 K in all degrees of freedom. Results for CID of ions produced in the flow tube are independent of the electron energy used in our experiments. They also do not change when the He flow rate is increased or when other gases such as SF_6 or Ar are added to the flow. These observations provide further evidence that the carbonyl ions are thermalized as they pass through the flow tube.

One possible complication in the ion production is the known propensity of metal ions to cluster with metal carbonyls.[24,53] This could be a problem in the present system since the most abundant isotope of iron, ^{56}Fe, has the same mass as two CO ligands. To diminish the probability of such clustering, the $Fe(CO)_5$ pressure in the FT was kept to less than 1 mTorr, the detectability limit of the capacitance manometer measuring the flow tube pressure. From the known characteristics of the valve used to admit the $Fe(CO)_5$, we estimate that its pressure in the flow tube was probably 1 order of magnitude less, i.e., ≪0.1% of the total pressure in the flow tube. No evidence for clustering such as secondary thresholds or enhanced loss of a 56-amu fragment was seen in any of the experiments described here. We have observed evidence of clustering reactions in our flow tube when a relatively large amount of $Fe(CO)_5$ is added.[54]

In one set of experiments described below, $Fe^+(^6D)$ was the reactant ion. For these, the flow tube was again used. Fe^+ is created by a cold cathode dc discharge, Figure 1. This source consists of a water-cooled metal rod isolated from ground and maintained at high negative voltage, typically 1–3 kV, by a Bertan Model 105 power supply. A cap of the desired metal target (carbon steel for these experiments) covers the end of the metal rod and acts as the cathode. A mixture of helium and argon (typically 5–7% Ar for these experiments) flows over the cathode and is ionized by the dc field. Neutral and ionic metal fragments are sputtered off the cathode by accelerated argon ions and entrained in the flow. Other neutral gases can be let in further downstream in order to ligate the metal ions or for additional cooling.

We have previously shown[55] that several thousand collisions of Fe^+ with Ar are sufficient to cool the ^4F first excited state to the ^6D ground state, and this was specifically verified for the flow tube source. O_2 was

(49) They derived a 298 K value of −179 kcal/mol by adding the enthalpy difference for $Fe(CO)_5$ (7.922 kcal/mol) without taking into account the enthalpy differences of the elements.

(50) Sugar, J.; Corliss, C. *J. Phys. Chem. Ref. Data, Suppl. No. 2* **1985**, *14*, 1.

(51) Ervin, K. M.; Armentrout, P. B. *J. Chem. Phys.* **1985**, *83*, 166.

(52) Leopold, D. G.; Murray, K. K.; Miller, A. E. S.; Lineberger, W. C. *J. Chem. Phys.* **1985**, *83*, 4849. Leopold, D. G.; Ho, J.; Lineberger, W. C. *Ibid.* **1987**, *86*, 1715.

(53) Kappes, M. M.; Staley, R. H. *J. Phys. Chem.* **1982**, *86*, 1332.

(54) Schultz, R. H.; Armentrout, P. B. Unpublished work.

(55) Elkind, J. L.; Armentrout, P. B. *J. Phys. Chem.* **1986**, *90*, 5736.

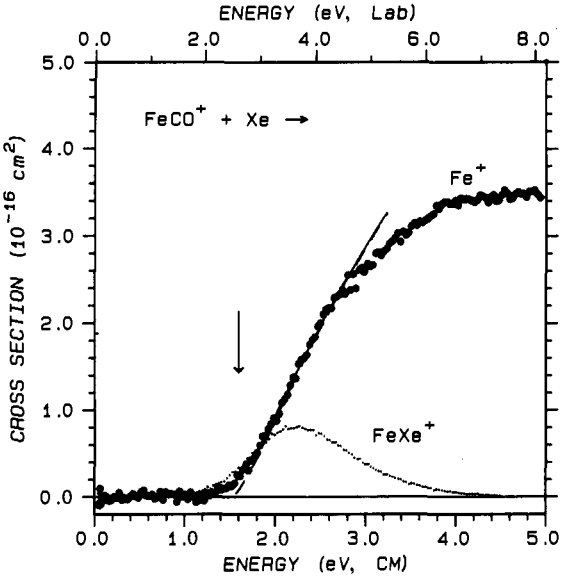

Figure 2. Cross sections for reaction of $FeCO^+$ with Xe as a function of relative kinetic energy (lower x axis) and laboratory energy (upper x axis). Solid circles show CID to form Fe^+, and the small dots show ligand exchange to form $FeXe^+$. The dashed line is a fit to the CID cross section that uses eq A1, and the solid line is the same fit convoluted over the ion and neutral translational energy distributions. The vertical arrow indicates the CID threshold of 1.59 eV.

added to the flow tube (approximately 3% of the total flow) to remove more highly excited Fe^+ ions, which react exothermically with O_2[56] and are thus removed. To ensure that the Fe^+ beam was thermalized, its reaction with O_2 was performed to make sure that there was no residual exothermic reaction. On the basis of the above tests and other work in our laboratory,[57] we estimate that the Fe^+ beam used for this study contains <2% excited states.

Data Analysis. Equation 2 gives the general form of the CID threshold excitation function, where E_0 is the threshold energy, σ_0 is an energy-independent scaling factor, E is the ion translational energy, and n is treated as a variable parameter. This form has been predicted for

$$\sigma = \sigma_0(E - E_0)^n/E \qquad (2)$$

CID processes,[58] and has been shown experimentally to provide accurate CID thresholds.[29,30,38] Before comparison with the experimental data, the calculated cross section is convoluted over the ion beam and neutral reactant energy distributions as described previously.[51] After the convolution, the variable parameters σ_0, E_0, and n are optimized by using a nonlinear least-squares analysis in order to best reproduce the data. We take the optimized value of E_0 to be the determined threshold for a particular data set. Uncertainties in the reported thresholds are derived from the spread of values for different data sets and the absolute uncertainty of the energy scale. For larger metal–ligand complexes, it is necessary to include effects of vibrational energy in the excitation function as discussed below.

Results

CID of $Fe(CO)_x^+$. Results for the interaction of $FeCO^+$ with Xe are shown in Figure 2. The major product is CID to form Fe^+, which rises from an apparent threshold below 1.5 eV. It reaches a maximum cross section of about 3.5 Å^2 above 4 eV, and does not decline appreciably below 7.5 eV. The other product observed is ligand exchange to form $FeXe^+$. This product has an apparent threshold slightly below that for CID, rises to a peak of about 1 Å^2 at 2 eV, and falls off quickly at higher energies. (The absolute magnitude of the product cross section has not been normalized for the isotopes of Xe, but the mass resolution of the quadrupole was sufficiently low that the cross section shown in Figure 2 represents the bulk of the product intensity for all isotopes.) No other products (i.e., FeC^+ or FeO^+) were seen, nor were any fragments containing unequal numbers of carbon and oxygen atoms observed from any of the larger carbonyl ions. Since an individual C–O bond is much stronger than even the sum of all five Fe^+–CO bonds, such an observation is unsurprising.

Results for the CID reaction of $Fe(CO)_2^+$ with Xe are shown in Figure 3. The main product is $FeCO^+$, which rises from an apparent threshold of about 1.5 eV to a peak cross section of about 10 Å^2 above 6 eV. Loss of two carbonyl ligands to form Fe^+ is

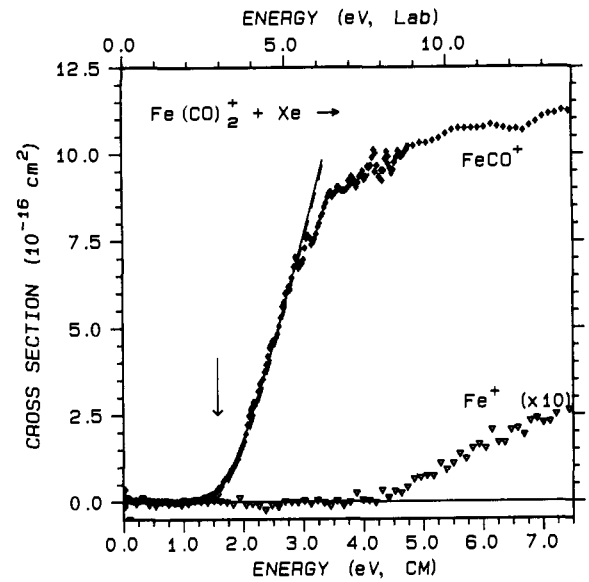

Figure 3. Cross sections for reaction of $Fe(CO)_2^+$ with Xe as a function of relative kinetic energy (lower x axis) and laboratory energy (upper x axis). Diamonds show cross sections for loss of one CO to form $FeCO^+$, and inverted triangles loss of two CO ligands to form Fe^+ (multiplied by 10). The vertical arrow indicates the threshold for loss of one CO at 1.57 eV. The dashed line is a fit to this data that uses eq A1 and this threshold. The solid line is the same fit convoluted over the ion and neutral translational energy distributions.

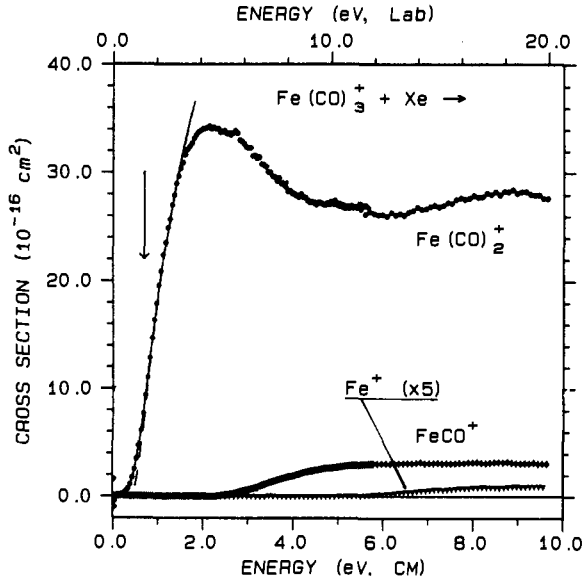

Figure 4. Cross sections for reaction of $Fe(CO)_3^+$ with Xe as a function of relative kinetic energy (lower x axis) and laboratory energy (upper x axis), extrapolated to zero pressure as described in the text. Circles show cross sections for formation of $Fe(CO)_2^+$, diamonds formation of $FeCO^+$, and inverted triangles formation of Fe^+ (multiplied by 5). The vertical arrow indicates the threshold for loss of one CO at 0.69 eV. The dashed line is a fit to this data that uses eq A1 and this threshold. The solid line is the same fit convoluted over the ion and neutral translational energy distributions.

(56) Loh, S. K.; Fisher, E. R.; Lian, L.; Schultz, R. H.; Armentrout, P. B. *J. Phys. Chem.* **1989**, *93*, 3159.
(57) Clemmer, D. E.; Chen, Y.-M.; Armentrout, P. B. Work in progress.
(58) Maier, W. B., II *J. Chem. Phys.* **1964**, *41*, 2174. Levine, R. D.; Bernstein, R. B. *Chem. Phys. Lett.* **1971**, *11*, 52. Rebick, C.; Levine, R. D. *J. Chem. Phys.* **1973**, *58*, 3942. Parks, E. K.; Wagner, A.; Wexler, S. *Ibid.* 5502. Viswanathan, R.; Raff, L. M.; Thompson, D. L. *Ibid.* **1983**, *79*, 2857. See also ref 29 and references therein.

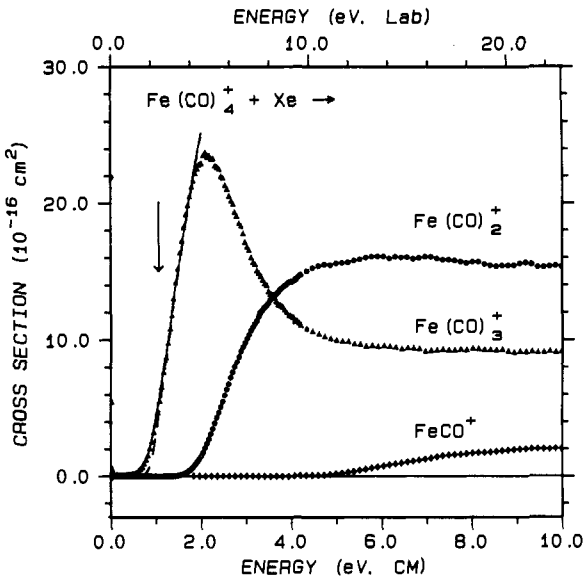

Figure 5. Cross sections for reaction of $Fe(CO)_4^+$ with Xe as a function of relative kinetic energy (lower x axis) and laboratory energy (upper x axis), extrapolated to zero pressure as described in the text. Triangles show cross sections for formation of $Fe(CO)_3^+$, circles formation of $Fe(CO)_2^+$, and diamonds formation of $FeCO^+$. The vertical arrow indicates the threshold for loss of one CO at 1.07 eV. The dashed line is a fit to the data that uses eq A1 and this threshold. The solid line is the same fit convoluted over the ion and neutral translational energy distributions.

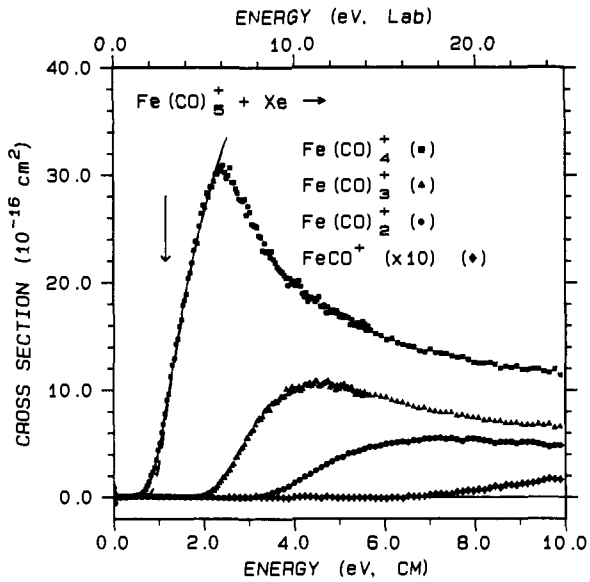

Figure 6. Cross sections for reaction of $Fe(CO)_5^+$ with Xe as a function of relative kinetic energy (lower x axis) and laboratory energy (upper x axis), extrapolated to zero pressure as described in the text. Squares show cross sections for formation of $Fe(CO)_4^+$, triangles formation of $Fe(CO)_3^+$, circles formation of $Fe(CO)_2^+$, and diamonds formation of $FeCO^+$ (multiplied by 10). The vertical arrow indicates the threshold for loss of one CO at 1.16 eV. The dashed line shows a fit to the data that uses eq A1 and this threshold. The solid line is the same fit convoluted over the ion and neutral translational energy distributions.

also observed at higher energy with a much lower probability (the peak cross section is <1 Å^2). While ligand exchange to form $Fe(CO)Xe^+$ is probably taking place, we cannot observe it (or, for that matter, ligand exchange with any of the larger reactant ions) because our detector quadrupole mass filter cannot measure m/z greater than about 200.

As shown in Figure 4, a significant change in behavior takes place with $Fe(CO)_3^+$. The apparent threshold for loss of the first CO is much lower, less than 1 eV, and the peak cross section is much larger, ~30 Å^2, than in the previous two systems. $Fe(CO)^+$ is observed with an apparent threshold of about 2 eV and a peak of ca. 5 Å^2. Fe^+ once again is seen only at high energy and with a peak cross section below 1 Å^2.

The CID spectrum of $Fe(CO)_4^+$ is shown in Figure 5. Once again, the behavior undergoes a change. The apparent threshold for loss of CO is higher than that for $Fe(CO)_3^+$, approximately 1 eV. Unlike the smaller species, in which the first daughter peak is the largest at all energies below 10 eV, the $Fe(CO)_3^+$ cross section peaks strongly below 2 eV and then falls below that for formation of $Fe(CO)_2^+$, which rises from a threshold of about 2 eV (i.e., where $Fe(CO)_3^+$ formation peaks, indicating that this product does *not* correspond to loss of Fe^+ from a putative $Fe_2(CO)_2^+$ ion) to peak at ~15 Å^2 above 4 eV. $FeCO^+$ and Fe^+ rise at higher energies with smaller cross sections than the other products.

Figure 6 shows the results for CID of $Fe(CO)_5^+$. Loss of one CO is similar to that from $Fe(CO)_4^+$; that is, the cross section rises from an apparent threshold of about 1 eV to a peak of about 25 Å^2. The cross section for formation of $Fe(CO)_3^+$ does not show the sharp peak it did from $Fe(CO)_4^+$, and does not cross that of $Fe(CO)_2^+$ until much higher energy, >10 eV.

$Fe^+(^6D)$ + $Fe(CO)_5$. We also ran the reaction of $Fe^+(^6D)$ with neutral $Fe(CO)_5$. Since the mass of the most abundant isotope of Fe has the same mass as two CO ligands, we ran these experiments using the ^{54}Fe isotope (5.82% natural abundance). We observed two major types of products, those of the form $^{56}Fe(CO)_x^+$ (x = 1-5) and those of the form $^{54}Fe^{56}Fe(CO)_x^+$ (x = 0-3). Ions containing more carbonyl ligands may also be formed, but due to the mass limitation of our detector mass spectrometer, we were unable to observe any of them. A very small amount of $^{54}FeCO^+$ was also observed. We did not observe any evidence

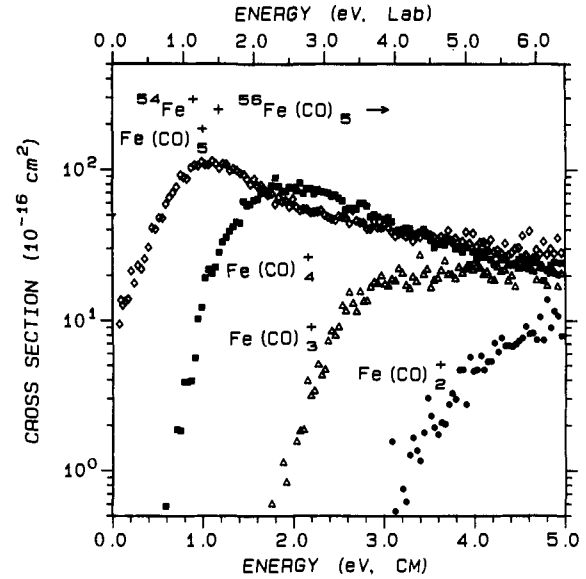

Figure 7. Cross sections for production of $^{56}Fe(CO)_x^+$ (x = 2-5) from reaction of $^{54}Fe^+(^6D)$ with $Fe(CO)_5$ as a function of relative energy (lower x axis) and laboratory energy (upper x axis). $Fe(CO)_5^+$ is shown as diamonds, $Fe(CO)_4^+$ as squares, $Fe(CO)_3^+$ as triangles, and $Fe(CO)_2^+$ as circles.

for transfer of more than one CO to the $^{54}Fe^+$. The intensity ratio of the $^{54}Fe^{56}Fe(CO)_x^+$ mass peaks to those two mass units below, which correspond to $^{54}Fe_2(CO)_x^+$ ions from ^{54}Fe in the neutral reagent, matched the $^{56}Fe/^{54}Fe$ abundance ratio, indicating that the $^{54}Fe^{56}Fe(CO)_x^+$ mass peaks did not contain any significant amount of $^{54}Fe(CO)_{x+2}^+$. The results for the $^{56}Fe(CO)_x^+$ products for x = 2-5 are shown in Figure 7.

Thermochemistry From CID Thresholds

Systematic Effects Affecting CID Threshold Measurements. It is one thing to make a precise measurement of a given unknown. It is another thing entirely to be sure that the precision is not compromised by systematic effects interfering with the accuracy of the measurement. Earlier work from our laboratory has dealt

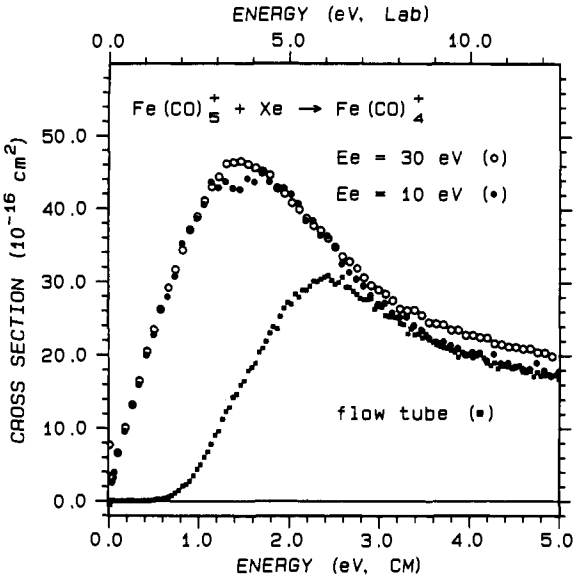

Figure 8. Cross sections for loss of one CO ligand by CID of $Fe(CO)_5^+$ created by electron impact ionization. The circles show results for $Fe(CO)_5^+$ made at electron energies of 30 eV (open circles) and 10 eV (closed circles). The closed squares are the data from Figure 6 (ions created in the flow tube) for comparison.

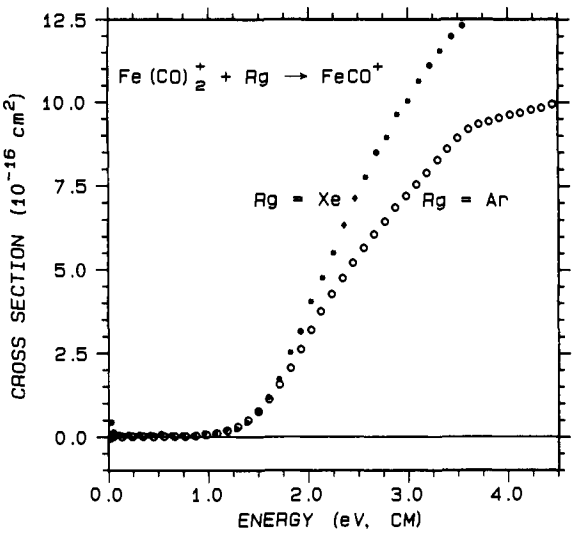

Figure 9. Cross sections for CID loss of one CO ligand from $Fe(CO)_2^+$ with different collision partners. Closed and open circles show CID by Xe and Ar, respectively.

with some of the possible systematic effects that can complicate the measurement of the true CID thresholds for transition-metal cluster ions. To our knowledge, investigations of possible systematic effects on CID thresholds of ligated metal systems have been limited in number and scope. Magnera et al.[34] did consider some possible systematic effects on their measurements of $Cu(H_2O)_x^+$ dissociation thresholds, such as different collision partners, internal energy carryover into products, and electronically excited parent ions. They concluded that their results were not systematically in error. Because Cu^+ has no low-lying excited electronic states, they concluded that they were measuring dissociation energies from ground state to ground state.

Because of the differences between our experimental setup and those of other researchers who perform CID measurements,[32,34] we decided to perform a careful investigation of possible systematic effects on our experiment. Here, we discuss four effects that we have previously observed to affect CID threshold measurements.

1. Internal Excitation of Reactant Ions. If the parent ions are created with an excess of internal energy, then the CID threshold can be shifted downward by this excess.[59] Since production of ions is necessarily an energetic process, care must be taken to cool the ions as much as possible. As shown in Figure 8, even "low"-energy electron impact ionization produces ions with significantly more internal energy than ions emitted from the flow tube source. Even the ions produced at an electron energy of only 10 eV, about 2 eV above the IE of $Fe(CO)_5$, Table II, show significant dissociation at a relative kinetic energy of zero. Clearly any thermodynamic data taken from ions generated under these conditions will be worthless.

Figure 8 shows, in addition, a more subtle complication. Since the data from the 10- and 30-eV electron energy conditions are the same to within experimental error, no *reactivity* test could tell them apart. While it might seem logical to assume that simply lowering the ionization energy until the ions exhibit no further change in reactivity would demonstrate that they are thermalized, a comparison with the flow tube data shows that this assumption is erroneous. A lack of change in reactivity with further cooling is a necessary but not a sufficient condition for showing that the ions are thermalized.

2. Effect of Collision Partner. Magnera et al.[34] reported that the choice of collision partner (Ar, Xe, or *n*-butane) had no effect on the results of their study of CID of $Cu(H_2O)_x^+$ systems. In contrast, we have previously observed in a number of systems[29,30,38] that the collision partner can affect CID threshold behavior. For CID of clusters containing main-group atoms,[30] charge transfer to a collision partner with a lower IE than the main-group atom can compete with and obscure CID. Of course, for $Fe(CO)_x^+$, that will not be a problem, since the IEs of all of the $Fe(CO)_x$ species are much lower than that of Xe.[17,23] The choice of collision partner, however, can make a difference in the threshold excitation function. Figure 9 shows CID of $Fe(CO)_2^+$ using Ar and Xe as the collision partners. While the location of the threshold appears to be the same for the two systems, the behavior at threshold is quite different, with the Ar-induced dissociation rising more slowly from threshold than that induced by Xe. This collision partner effect has been observed before in other transition-metal ion systems.[29,59] We have explained this behavior in terms of the amount of time available for energy transfer during the reactive encounter. As the neutral reactant gets lighter, the lab energy necessary to yield a given CM energy increases. That means that there is less time available to the reactants to interact and the probability of efficient $T \rightarrow V$ energy transfer necessary for CID decreases. Thus, for the lighter collision partner, the reaction probability rises more slowly from the threshold, making accurate determination of the threshold more difficult. For this reason, all of the threshold measurements reported here are from experiments that used Xe as the neutral reactant.

3. Pressure Effects. Initially, we performed the CID experiments at as low a pressure in the gas cell as the reaction region capacitance manometer could accurately read, ca. 0.05 mTorr. Such conditions are essentially "single collision", and are expected to lead to accurate thresholds. There is, however, always some finite probability of a second collision as soon as there are two neutral gas molecules in the gas cell. Our studies of transition-metal cluster ion CID have shown that multiple collisions can strongly affect CID threshold behavior.[38] Such an effect can occur if a polyatomic ion were, for instance, to undergo two collisions at half the actual BDE, and if all of the energy of the collisions were to go into internal excitation of the ion. In such a case, the ion would appear to have dissociated at a translational energy only half of the true thermodynamic threshold.

Figure 10 shows the pressure dependence for loss of one and two carbonyls from $Fe(CO)_4^+$. Even at the lowest pressure shown, where the probability of a single collision is less than 5% and that of two collisions is only ~0.3%, there is an observable shift in the dissociation threshold to lower energies. The most effective way to eliminate this effect is to extrapolate the behavior to zero pressure. If the threshold shift is due to double collisions, then a linear extrapolation will be sufficient, while if more collisions are taking place, then the extrapolation will have to include more

(59) Hales, D. A.; Armentrout, P. B. *J. Cluster Sci.* **1990**, *1*, 127.

Table III. Measured $(CO)_{x-1}Fe^+$–CO BDEs (eV)[a]

parent ion[b]	$D_0°[(CO)_{x-1}Fe^+–CO]$				
	x = 1	x = 2	x = 3	x = 4	x = 5
$Fe(CO)^+$	1.42 ± 0.13				
	1.49 ± 0.13				
	1.59 ± 0.08				
$Fe(CO)_2^+$	1.90 ± 0.14	1.37 ± 0.07			
		1.47 ± 0.07			
	2.03 ± 0.41	**1.57 ± 0.05**			
$Fe(CO)_3^+$	2.32 ± 0.61	1.74 ± 0.08	0.40 ± 0.03		
	2.15 ± 0.89	*2.08 ± 0.15*	*0.43 ± 0.04*		
			0.59 ± 0.04		
	1.90 ± 1.03	**1.95 ± 0.14**	**0.69 ± 0.05**		
$Fe(CO)_4^+$		1.87 ± 0.57	0.95 ± 0.20	0.69 ± 0.06	
		2.92 ± 0.24	*1.22 ± 0.12*	*0.73 ± 0.03*	
				0.95 ± 0.03	
		2.89 ± 0.23	**1.14 ± 0.12**	**1.07 ± 0.06**	
$Fe(CO)_5^+$			0.51 ± 0.22	1.19 ± 0.11	0.69 ± 0.06
			1.16 ± 0.19	*2.15 ± 0.18*	*0.79 ± 0.06*
					1.07 ± 0.06
			1.24 ± 0.14	**1.42 ± 0.13**	**1.16 ± 0.04**

[a] Thresholds determined by using eqs 2 and A1. Numbers in roman type represent fits to the data that use threshold models that are not corrected to zero pressure and do not consider vibrational effects. Numbers in italics represent fits to data that are corrected to zero pressure, but without any consideration of the vibrational energy of the parent ion. Underlined numbers are the previous numbers "corrected" by simply adding the average vibrational and rotational energy to the observed threshold (see text). Numbers in boldface are from analyses of pressure-corrected data that use eq A1 in which the vibrational energy of the ions is explicitly considered in the threshold model and the rotational energy has been added in as well. The rightmost column for each parent ion gives the values of the thresholds for loss of one CO. The other columns are BDEs derived from differences between the thresholds for formation of $Fe(CO)_x^+$ and $Fe(CO)_{x-1}^+$. [b] The cross sections for dissociation products of $FeCO^+$ and $Fe(CO)_2^+$ are independent of the pressure of Xe in the gas cell.

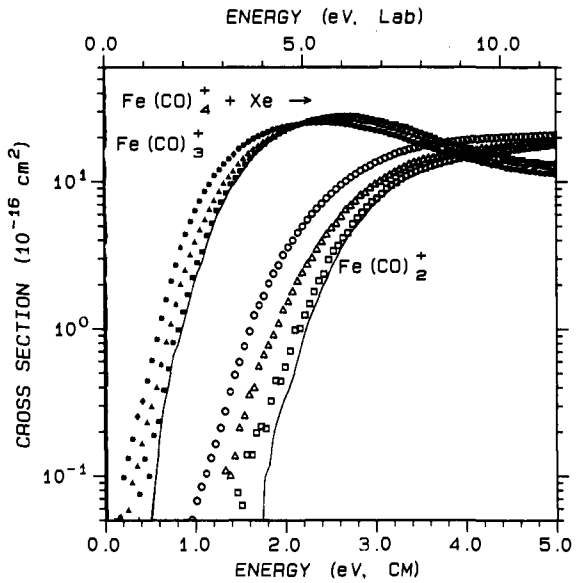

Figure 10. Pressure dependence of the threshold cross sections for loss of one (closed symbols) and two (open symbols) CO ligands from $Fe(CO)_4^+$. Circles, triangles, and squares show cross sections for CID experiments performed at gas cell pressures of 0.38, 0.16, and 0.04 mTorr, respectively. The solid lines show the linear extrapolations of these cross sections to zero pressure. The cross sections are plotted on a logarithmic *y* axis to show the effect more clearly.

terms. To make sure that this pressure effect is due only to two (but no more) collisions, experiments were performed at several different pressures. No significant differences were found between extrapolations from any two data sets and a linear extrapolation that included all of them. Therefore, most experiments were done at only two pressures (typically differing by a factor of 6–8).

Pressure effects are not significant for $FeCO^+$ and $Fe(CO)_2^+$, but are very much so for the larger ions. The lowering of the thresholds as pressure is increased becomes more obvious for loss of more than one CO ligand, as shown in Table III and Figure 10. Because this pressure effect is not quantitatively the same for loss of different numbers of ligands, BDEs measured as the difference between such thresholds will be pressure dependent. The implications of these threshold shifts for the use of secondary thresholds to determine thermochemistry will be discussed in more detail below.

4. Lifetime Effects. One other possible effect on the thresholds for dissociation is the finite time available to the dissociating ion as it tranverses the instrument from the reaction region to the detector. For a sufficiently large ion, the amount of time available to it (ca. 10 μs in our apparatus) may be less than the time it takes for the energy to be distributed into the reaction coordinate to cause bond rupture. We have observed this problem for large transition-metal clusters on an instrument similar to the one on which these experiments were performed. For these cases, we use an RRKM procedure to model these lifetime effects.[39] To ensure that lifetime effects are not a problem in the current system, we use this RRKM routine to model the CID excitation function for $Fe(CO)_5^+$, the worst case. The calculated cross sections were indistinguishable whether or not the RRKM routine was included in the calculation, indicating that the lifetimes of the ions studied here are short enough that primary dissociation occurs within the experimental time scale.

Thermal Energy Effects. Having taken the factors discussed above into account, we thought that the resulting data should give accurate $Fe(CO)_x^+$ BDEs. Results for CID of flow tube cooled ions with Xe (the first entries in Table III) yield $\Delta_r H°(1)$ = 105 ± 4 kcal/mol. After extrapolating to zero pressure, this heat of reaction increases by only 4 kcal/mol to 109 ± 4 kcal/mol, still disappointingly low compared with the literature value of 136.4 ± 1.9 kcal/mol. This low value is not due to any obvious failure of eq 2 to reproduce the data, as shown by the typical analysis given in Figure 11a.

One possible explanation for the low value of $\Delta_r H°(1)$ is that the reactant ions are not truly thermal, leading to dissociation below the true thermodynamic threshold. There are several reasons why this explanation is unlikely for the present experiments. First, the method of producing the ions should cool them, since they undergo about 10^5 collisions with He and Ar and have plenty of time (tens to hundreds of microseconds) to lose any large amount of excitation in the form of ejected CO molecules. Second, the systematic effects discussed above affect the dissociation thresholds of larger ions more than those of the smaller ones, Table III. Since the larger ions have more degrees of freedom and more low-frequency bending and stretching vibrational modes, we would expect them to be cooled more, not less, effectively under our

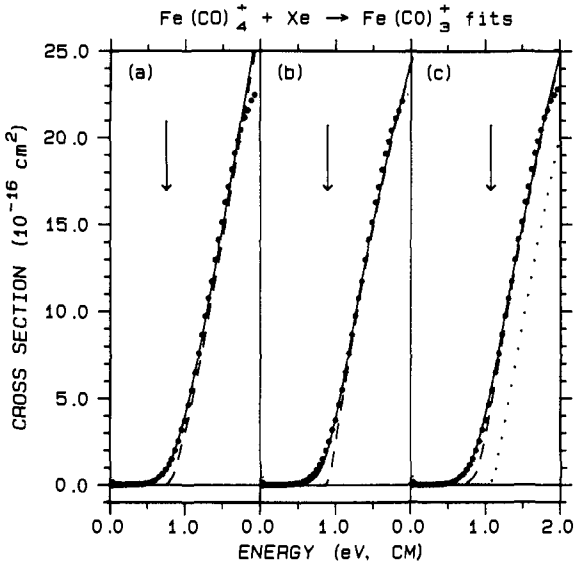

Figure 11. Cross sections in the threshold region for loss of one CO ligand from $Fe(CO)_4^+$, same data as Figure 5. Part a shows a fit to the data using eq 2 with $E_0 = 0.75$ eV and $n = 1.9$. Part b shows the same data with a fit that uses eq 2 but ignores the lowest energy points and has $E_0 = 0.89$ eV and $n = 1.4$. Part c shows the same data fit by using eq A1 that takes into account the vibrational energy distribution at 300 K of the parent ion and has $E_0 = 1.07$ eV and $n = 1.4$. For all three fits, the model cross section given by the appropriate equation is shown as a dashed line, and the same fit convoluted over the ion and neutral translational energy distributions is shown as a solid line. The dotted line in part c shows the unconvoluted model cross section ($E_0 = 1.07$ eV) for the ground vibrational state only. The vertical arrows indicate the respective CID thresholds.

source conditions. Third, the threshold behavior does not change even when the source conditions are made more severe than usual, either by lowering the electron energy, increasing the He pressure by 20%, or adding SF_6 to the flow. It seems likely then that the low value of $\Delta_f H°(1)$ is something inherent even in the thermalized ions.

Even if the ions are thermalized, there is one effect that could lead to spuriously low values for the CID thresholds, namely, vibrational energy coupling with the dissociation reaction coordinate. In other words, if the reactant ions are at 300 K, but the products at threshold are at 0 K, then the thermal vibrational energy will lower the observed threshold below its true 300 K value. One simple way of dealing with this problem is to add the average vibrational and rotational energy to the threshold obtained by fitting the data as in Figure 11a. For the case of the $Fe(CO)_5^+$, the average amount of vibrational excitation at 300 K is nearly 0.25 eV, as calculated by assuming a Maxwell–Boltzmann population and the vibrational frequencies given by ref 3. For the smaller ions, we simply removed frequencies corresponding to the appropriate number and types of vibrational modes lost with each CO and recalculated the energies by using this first approximation. As can be seen from Table III, this method, which yields a value for $\Delta_f H°(1)$ of 128.2 ± 3.9 kcal/mol, comes closer to the correct value although it is still too low. Thus, the thresholds produced for this system by eq 2 are not simply the true thermodynamic thresholds lowered by an amount corresponding to the available energy. Apparently, the model of eq 2 cannot approximate the true thermodynamic thresholds for such metal–ligand complexes where there are numerous "floppy" degrees of freedom.

If eq 2 truly is incapable of handling the details of the threshold excitation functions for the CID of such molecules, then it may be more justifiable to fit the data in nontraditional ways. For example, one temporary solution that we attempted was to fit only the steeply rising portion of the excitation function and ignore the points near threshold. Figure 11b shows an example of such a fit for loss of one CO from $Fe(CO)_4^+$. This treatment of the data yields a value for $\Delta_f H°(1)$ of 130 ± 5 kcal/mol and bond strengths of about 1 eV for $(CO)_3Fe^+$–CO and $(CO)_4Fe^+$–CO and about 0.6 eV for $(CO)_2Fe^+$–CO. Higher BDEs are obtained because the optimal form of eq 2 has lower values of the parameter n, typically $n = 1.3$–1.6, compared to the typical values of $n = 1.6$–2.0 for $(CO)_3Fe^+$–CO and $(CO)_4Fe^+$–CO obtained above. The values of n and E_0 are coupled such that a higher value of n yields a cross section that rises more slowly from a lower threshold. While ignoring the data points near the threshold may offer an empirical approach to obtaining reasonable thermochemistry, such a method of fitting the data is unsatisfying because eq 2 has been found to be adequate for a wide range of experimental systems including CID[29,38] and is theoretically justified as well.[58] Furthermore, ignoring data in the critical threshold region begs the question of why the threshold model fails.

The comparisons above demonstrate that the cross section model of eq 2 cannot simultaneously reproduce the slowly rising part of the cross section at threshold and yield the correct BDE for these systems. This failure is clearly due to the nonzero vibrational energy of the ions that contributes to a lowering of the measured threshold. The most appropriate (and most difficult) approach to modeling the CID behavior of these polyatomic ions is to explicitly consider the entire distribution of vibrational states populated rather than ignoring it or simply adding the average vibrational energy as described above. To this end, we have developed such a multistate model, eq A1, the mathematical details of which are described in the Appendix. When this model rather than eq 2 is used, the data are reproduced well throughout the threshold region as shown in Figure 11c. As expected according to the line of argument given above, the multistate model utilizes lower values of n (typically 1.3–1.5) and obtains a value for $\Delta_f H°_0(1)$ that is within experimental error of the literature value.

Bond Dissociation Energies. 1. $(CO)_xFe^+$–CO BDEs from Primary Thresholds. With the inclusion of vibrational energy in the fitting model, we now get a series of bond strengths whose total of 140.0 ± 3.1 kcal/mol is within combined experimental error of the literature value of $\Delta_f H°_0(1)$, 136.4 ± 1.9 kcal/mol. Since we have explicitly included the internal energy of the reactant ion, these bond strengths are therefore already corrected to 0 K. All of the bond strengths we recommend come from the primary thresholds, which are the most precise, least susceptible to kinetic shifts, and least ambiguous. We therefore recommend the values summarized in Table III. The trends in the bond strengths and possible complications of electronic effects are discussed below.

2. $(CO)_xFe^+$–CO BDEs from Secondary Thresholds. In principle, one should be able to determine thermochemistry from the differences in the thresholds for loss of successive CO ligands. Specifically, the difference between the thresholds for formation of $Fe(CO)_y^+$ and formation of $Fe(CO)_{y-1}^+$ is just the $(CO)_{y-1}Fe^+$–CO BDE. Indeed, differences between thresholds for secondary dissociation have been used to determine successive BDEs for $M(H_2O)_x^+$[34] and $Mn_2(CO)_x^+$.[60] It might be thought that such a method is more reliable since it should lead to a cancellation of systematic errors. As can be seen from Table III, however, this method must be used with caution. For the secondary thresholds measured with no pressure correction, some "BDEs" determined this way, for instance, $(CO)_3Fe^+$–CO from $Fe(CO)_5^+$, are in reasonable agreement with those determined from the primary thresholds. For many of the others, however, the agreement is much worse. The secondary thresholds obtained from data extrapolated to zero pressure are uniformly in bad agreement with those obtained from the primary thresholds. The poor agreement stems from the difficulty of accurately modeling the cross sections, which rise quite slowly from threshold. Many of them show every sign of having a kinetic shift as well, as postulated for the ions arising from loss of more than one CO in the PI experiments. Such kinetic shifts are particularly obvious for products that represent loss of several CO ligands, e.g., $FeCO^+$ formation from $Fe(CO)_5^+$, which has a thermodynamic threshold of 4.5 eV yet appears to arise from a threshold of ~6.5 eV, Figure 6. This kinetic shift may explain why some of the values obtained

(60) Yu, W.; Liang, X.; Freas, R. B. *J. Phys. Chem.* **1991**, *95*, 3600.

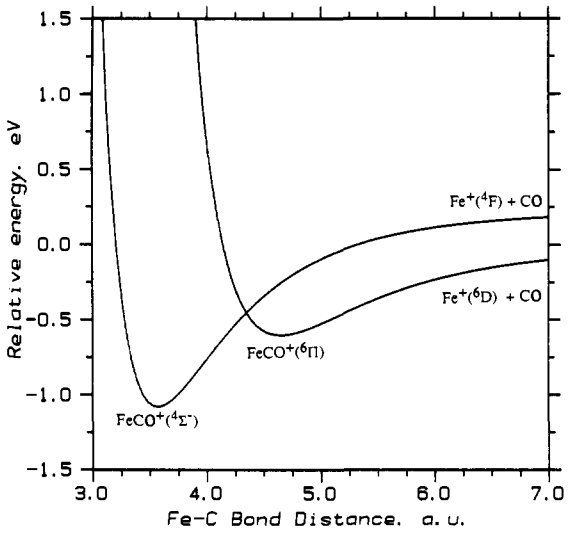

Figure 12. Lennard-Jones potential energy surfaces for dissociation of $FeCO^+(^4\Sigma^-)$ and $FeCO^+(^6\Pi)$. The equilibrium Fe^+–C distances and D_e values are taken from ref 11.

from the unextrapolated data sets turn out to be accurate. In these cases, the two systematic effects (higher threshold due to a kinetic shift vs lower threshold due to multiple collisions) that work in opposite directions serve to cancel one another to the extent that the net result is in reasonable agreement with that determined directly from the primary CO loss. In general, while secondary thresholds may yield qualitatively reasonable thermochemistry in CID of ligated metal ions, it is clear that they cannot necessarily be relied upon to provide quantitatively accurate BDEs.

3. Fe^+–Xe. We can also determine a BDE for the ligand exchange product, $FeXe^+$, from the difference between the CID and ligand exchange thresholds for $FeCO^+$. We observe a threshold for ligand exchange of 1.17 ± 0.05 eV, and thus obtain a value of 0.39 ± 0.09 eV (9.0 ± 2.0 kcal/mol) for the Fe^+–Xe bond strength. This value is much lower than the V^+–Xe BDE of 0.84 ± 0.17 eV measured by Aristov and Armentrout.[29] The difference is presumably due primarily to the additional electrons (especially the occupied 4s orbital) on Fe^+ increasing the repulsive interaction between the metal and ligand electron shells. We have measured similar values for the Fe^+–Xe bond strength from ligand exchange with H_2O and small alkanes.[35]

Discussion

Diabatic vs Adiabatic Dissociation of Fe^+–CO. As mentioned above, Barnes et al.[11] have calculated that the ground state of $FeCO^+$ is a quartet. This means that it will dissociate diabatically to the first excited ^4F state of Fe^+ rather than to ground-state $Fe^+(^6D)$. Barnes et al. predicted that, for PI and EI experiments, it is likely that dissociation will follow the diabatic path to $Fe^+(^4F)$ rather than the adiabatic path to $Fe^+(^6D)$. They also calculated that D_e should be 36.1 kcal/mol (which after correction for zero-point energy yields D_0° = 34.9 kcal/mol), while adiabatic dissociation has a D_e = 30.3 kcal/mol (D_0° = 29.1 kcal/mol). Their calculations are generally low by a couple of kilocalories per mole, which would put our measured CID threshold for Fe^+–CO squarely in line with it being the diabatic rather than the adiabatic threshold. Furthermore, their calculated value for $D_e(COFe^+$–CO), 34.5 kcal/mol (D_0° = 33.1 kcal/mol), is in quite good agreement with our experimental value. Unfortunately, the calculations and our threshold are not precise enough to determine unambiguously which dissociation of Fe^+–CO we are observing.

We can make some informed conjecture, however, given the evidence before us. Figure 12 shows potential energy surfaces for dissociation of Fe^+–CO in these two low-lying states based on the calculations of Barnes et al.[11] The diagram clearly shows that there is a surface crossing between the two states. In order for $FeCO^+$ to undergo adiabatic dissociation, the molecule must make the crossing after a single collision with Xe has energized it. While such a crossing is possible, it is not expected to be very likely. We have previously shown that about 1000 collisions between Fe^+ and Ar are necessary to relax $Fe^+(^4F)$ to $Fe^+(^6D)$.[55] Since CO and Ar have similar polarizabilities,[61] we might expect the Fe^+–CO system to have a similar low probability for making the surface crossing to the sextet surface. If the crossing has less than a 0.1% chance of being made, we would not be able to observe its effect on our measured threshold. Of course, the potential energy surfaces for the interaction of $Fe^+(^6D,^4F)$ with Ar[62] have been calculated to have smaller well depths and longer bond distances than those for $Fe^+(^6D,^4F)$ with CO,[11] but the qualitative aspects of this comparison can serve as a guide to understanding the surface crossing probabilities.

Further evidence for diabatic dissociation is that the D°-(Fe^+–CO) = 26 ± 5 kcal/mol measured by van Koppen et al.[22] is in good agreement with the value we measure here if we take our CID threshold to be that for formation of $Fe^+(^4F)$. These researchers noted that the kinetic energy release distribution (KERD) of $FeCO^+$ formed in the reaction of Fe^+ with acetone is bimodal and difficult to fit by using statistical phase space theory. This result suggests that they may have been observing formation of both sextet and quartet Fe^+.

If we assume then that we are observing the diabatic threshold, then the adiabatic threshold is lower at 0 K by 5.35 kcal/mol; i.e., the true BDE of Fe^+–CO is actually 31.3 kcal/mol, and the value that we obtain for $\Delta_f H^\circ(1)$ is 134.8 ± 3.0 kcal/mol. This value is actually in closer agreement with the literature number than that derived using the higher value for Fe^+–CO above. Thus, while we cannot unambiguously state which dissociation we are observing, it seems likely that we are actually observing the diabatic dissociation to $Fe^+(^4F)$.

Comparison to Previous BDE Determinations. Our values for the individual BDEs are consistent with the limits determined by the studies of Cassady and Freiser[20] and Tecklenberg et al.[21] With the exception of $(CO)_4Fe^+$–CO, they are within combined experimental error of Distefano's values[17] as corrected by Halle et al.[19] and, as described above, in good agreement with the calculated values of Barnes et al.[11] for $D^\circ(Fe^+$–CO) and $D^\circ[(CO)Fe^+$–CO]. Our agreement with the individual values determined by NAFN is not as good, although the values measured for $D^\circ(Fe^+$–CO) and $D^\circ[(CO)_3Fe^+$–CO] agree within combined experimental error. We have already discussed the inconsistency between the value they obtained for $\Delta_f H^\circ(1)$ and the literature value and how the source of the discrepancy is probably a kinetic shift affecting the threshold for appearance of Fe^+.

It is more difficult to understand why our value for $(CO)_4Fe^+$–CO is in such poor agreement with the two appearance potential energy measurements. In those experiments, we might expect the $(CO)_4Fe^+$–CO BDE to be the most accurate one. The most likely explanation is that both Distefano and NAFN are observing the same vibrational effects that led to the low value for our initial measurement of $(CO)_4Fe^+$–CO. In fact, if we do not take vibrational energy into account, our pressure-extrapolated data yield a value of 18.2 ± 1.4 kcal/mol for this BDE, Table III, in excellent agreement with the two appearance potential measurements. As Distefano's measurement was made at 298 K, it is not surprising that he observed thermal vibrational effects. That NAFN obtained a similar result suggests that, under the conditions of their supersonic expansion, vibrational degrees of freedom may not have been cooled very efficiently.

The above line of argument also implies that all of the PI thresholds have been shifted to lower energies. Since the PI experiments derive the BDEs as differences between thresholds, the bond energies for subsequent CO loss remain unchanged. Thus, the values of $D_0^\circ[(CO)_3Fe^+$–CO] obtained by the CID and PI experiments are in good agreement, Table I. Subsequently, bond energies derived by PI are higher than our CID results, presumably due to kinetic shifts in the PI experiments that obscure

(61) Rothe, E. W.; Bernstein, R. B. *J. Chem. Phys.* **1959**, *31*, 1619.
(62) Bauschlicher, C. W., Jr.; Partridge, H.; Langhoff, S. R. *J. Chem. Phys.* **1989**, *91*, 4733.

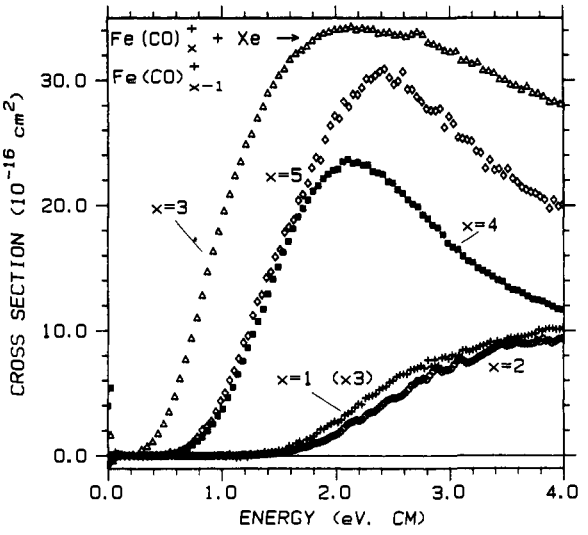

Figure 13. Cross sections for loss of one CO ligand for all five $Fe(CO)_x^+$ ions studied here.

the true thresholds for these highly dissociated product ions. Likewise, whereas the sum of the five BDEs obtained by the PI experiments should be too low if the vibrational energy contributes, kinetic shifts explain why the PI experiments obtain higher values of $\Delta_f H°(1)$.

The IE of $Fe(CO)_5$. NAFN's recent remeasurement of the IE of $Fe(CO)_5$ (ref 23) provided values lower than those previously accepted in the literature. While we have thus far simply taken the average of all of the literature measurements for calculating thermochemistry, we have also some evidence that the IE of $Fe(CO)_5$ is at the upper end of the literature values. As can be seen from Figure 7, the charge-transfer reaction from Fe^+ to $Fe(CO)_5$ is apparently endothermic, rising steeply as the energy is increased, although there is significant reactivity even at zero energy. Since the IE of Fe is well-established as 7.9024 ± 0.0001 eV,[50] our observation implies that $IE[Fe(CO)_5] > 7.90$ eV. A fit to the data shown in Figure 7 for the charge-transfer reaction yields a threshold of 0.035 ± 0.035 eV, implying that $IE[Fe(CO)_5] = 7.94 \pm 0.04$ eV, in good agreement with the earlier PI results and with the value chosen in the Introduction.

Trends in BDEs. Figure 13 shows loss of one CO from all five $Fe(CO)_x^+$ ions studied here. This figure makes graphically clear the trends shown in Table III: The Fe^+–CO and $(CO)Fe^+$–CO bonds are of nearly equal strength, the $(CO)_3Fe^+$–CO and $(CO)_4Fe^+$–CO bonds are weaker than these but of similar strength to each other, and the $(CO)_2Fe^+$–CO BDE is much weaker than any of the others. The unusual weakness of the third CO BDE deserves further comment. It is very unlikely that the low BDE for this one ligand is an experimental artifact. Not only would a higher BDE put our results in conflict with the established literature thermochemistry, but the EI mass spectra of $Fe(CO)_5$ also support a peculiar weakness to $Fe(CO)_3^+$. Distefano[17] cites five EI mass spectra of $Fe(CO)_5$ done at electron energies ranging from 21 to 50 eV and temperatures from room temperature to 250 °C. In all five cases, $Fe(CO)_3^+$ is the least abundant ion of the $Fe(CO)_x^+$ ions ($x = 0$–5) in the mass spectrum. Further, the dissociation behavior of $Fe(CO)_4^+$, Figure 5, makes it clear that $Fe(CO)_3^+$ is relatively unstable, as the cross section for formation of $Fe(CO)_2^+$ (loss of two CO ligands) actually is greater than that of $Fe(CO)_3^+$ above 3.5 eV (loss of one CO ligand). All of this evidence points to a particularly weak $(CO)_2Fe^+$–CO BDE.

One way of approaching the question of why this bond should be so weak is to consider the spin of the $Fe(CO)_x^+$ ions. Since $Fe(CO)_5$ has a full valence shell, and hence is a singlet, $Fe(CO)_5^+$ is likely to be a doublet. As discussed above, theoretical calculations[11] have shown that both $Fe(CO)^+$ and $Fe(CO)_2^+$ have quartet ground states. Therefore, there must be a spin change somewhere in between. The dissociation behavior of $Fe(CO)_3^+$ is consistent with the spin change occurring with the loss of its first ligand; that is, $Fe(CO)_3^+$ is postulated to have a doublet spin ground state that efficiently dissociates along the adiabatic pathway to the quartet spin ground state of $Fe(CO)_2^+$. This type of pathway would occur on potential energy surfaces analogous to those shown in Figure 12 for dissociation of $FeCO^+$. Thus, $Fe(CO)_3^+$ has a relatively weak BDE since it can dissociate adiabatically to the lower energy quartet spin asymptote, while $Fe(CO)_5^+$ and $Fe(CO)_4^+$ have relatively strong BDEs since they are postulated to have doublet ground states that dissociate diabatically and adiabatically along doublet spin surfaces. This hypothesis may be contrasted with the neutral $Fe(CO)_x$ species in which magnetic circular dichroism studies have shown that $Fe(CO)_4$ is a triplet.[63]

A rationale for why the spin change occurs with $Fe(CO)_3^+$ concerns the participation of the valence p orbitals in the metal carbonyl bonding. Because the valence p orbitals on the metal ion are too high in energy to take part in the bonding easily, unsaturated gas-phase ligated ions can have full valence shells consisting of 12 (the valence s and d orbitals) rather than 18 electrons. This qualitative idea is in good accord with more quantitative predictions of Barnes et al. on $M(CO)^+$ and $M(CO)_2^+$ bonding.[11,64] Since $Fe(CO)_3^+$ is a 13-electron species, it can form a doublet state by including the valence p orbitals and paying the promotion energy costs, resulting in a relatively weak BDE. $Fe(CO)_4^+$ and $Fe(CO)_5^+$, 15- and 17-electron complexes, respectively, will have stronger bonds since the energetic cost of including the valence p orbitals has already been paid.

Dearden et al.[65] used KERD analysis to determine the gas-phase $(CO)_xMn^+$–CO BDEs. The Mn^+ system is analogous to the Fe^+ system in that both ionic systems must undergo several spin changes to get from the ground state of the most ligated ion to the bare metal (singlet to septet for Mn^+ as opposed to doublet to sextet for Fe^+). The BDEs that they determined by fitting phase-space calculations to the KERDs also show a nonmonotonic progression, which presumably arises from analogous spin considerations to those discussed above for the $Fe(CO)_x^+$ system. For instance, $D°[(CO)_5Mn^+–CO]$ and $D°[(CO)_2Mn^+–CO]$ were about 30 kcal/mol, greater than either $D°[(CO)_4Mn^+–CO]$ or $D°[(CO)_3Mn^+–CO]$, both of which were about 20 kcal/mol. It is clear that monotonically increasing or decreasing BDEs are not necessarily to be expected for transition-metal carbonyl systems.

Conclusions

Our CID study of the $Fe(CO)_x^+$ ions has shown that CID can provide accurate bond dissociation energies for gas-phase ligated metal systems. The total of the five bond strengths obtained here, 140.0 ± 3.1 kcal/mol (or 134.8 ± 3.1 kcal/mol if $FeCO^+$ dissociates diabatically to $Fe^+(^4F)$ rather than adiabatically to $Fe^+(^6D)$), is in good agreement with the established literature thermochemistry. The individual bond strengths are generally (although not always) within experimental error of prior photoionization measurements. The differences in the BDEs determined by the present CID measurements and those from prior PI studies are primarily due to kinetic shifts in the PI thresholds and differences in experimental conditions. Because we measure all five iron–carbonyl bond energies in exactly the same fashion, via primary CID thresholds, the BDEs measure here are more likely to be free from such interferences.

We have also identified several possible sources of systematic error in CID studies, and shown that accurate measurement of CID thresholds depends on understanding and controlling all of these possible sources of error. The $Fe(CO)_x^+$ system has served as a useful prototype for CID of ligated metals and as a demonstration that, for CID thresholds to be measured accurately in larger systems, the vibrational energy available from the parent

(63) Barton, T. J.; Grinter, R.; Thomson, A. J.; Davies, B.; Poliakoff, M. *J. Chem. Soc., Chem. Commun.* **1977**, 841.
(64) Barnes, L. A.; Bauschlicher, C. W., Jr. *Chem. Phys.* **1988**, *124*, 383. Mavridis, A.; Harrison, J. F.; Allison, J. *J. Am. Chem. Soc.* **1989**, *111*, 2482.
(65) Dearden, D. V.; Hayashibara, K.; Beauchamp, J. L.; Kirchner, N. J.; van Koppen, P. A. M.; Bowers, M. T. *J. Am. Chem. Soc.* **1989**, *111*, 2401.

Table IV. Vibrational Frequencies (cm^{-1}) Used for Modeling the Thresholds of $Fe(CO)_x^+$ Ion CID (Degeneracies in Parentheses)

ion	frequencies
$Fe(CO)_5^+$	74.3 (2), 97.3 (2), 100, 104.9 (2), 375 (2), 383, 413.4, 429, 442.8, 474.3 (2), 488 (2), 542.5 (2), 618.8, 645 (2), 2013.3 (2), 2041.7, 2034, 2120.7[a]
$Fe(CO)_4^+$	A: 74.3 (2), 100, 104.9 (2), 375 (2), 383, 429, 442.8, 474.3 (2), 488, 542.5 (2), 618.8, 645, 2013.3 (2), 2034, 2120.7
	B: 92 (5), 435 (8), 450 (4), 2000 (4)
	C: 100 (5), 450 (4), 600 (8), 2000 (4)
	D: 100 (5), 400 (4), 600 (8), 2000 (4)
$Fe(CO)_3^+$	A: 100 (3), 400 (3), 500 (6), 2000 (3)
	B: 50 (3), 250 (3), 300 (3), 400 (3), 2200 (3)
$Fe(CO)_2^+$	A: 50 (2), 200, 300 (5), 2400 (2)
	B: 40 (2), 150, 250 (5), 2380 (2)
	C: 66 (2), 200 (2), 300 (4), 2300 (2)
$FeCO^+$	50, 250 (2), 2400

[a] Reference 3.

ion must be taken into account explicitly in the threshold model used.

Acknowledgment. This research was supported by the National Science Foundation, Grant No. CHE-8917980.

Appendix

Thresholds for Polyatomic Ions. Cross section thresholds for CID of polyatomic ions are modeled by using eq A1, where the single term of eq 2 is replaced by a summation over the vibrational states i having relative populations of g_i, where $\sum g_i = 1$. We

$$\sigma = \sigma_0 \sum g_i (E + E_i - E_0)^n / E \qquad \text{(A1)}$$

assume that the relative reactivity of each state is the same; i.e., $\sigma_{i0} = \sigma_0$ for all states i. The resulting model cross section is then convoluted over the ion and neutral translational energy distributions as described above. This model for vibrational states is, except for the method of deriving the populations and energy levels, the same as the method we use to fit ion–molecule reactions for atomic ions with multiple electronic states which has been described elsewhere.[66]

We derive the relative vibrational state populations and energy levels for inclusion in eq A1 as follows. The vibrational density of states of the polyatomic ion is first calculated by using the Beyer–Swinehart algorithm,[67] and then the appropriate Maxwell–Boltzmann distribution at 300 K is calculated. The resulting distribution of energies and vibrational modes is then divided into a maximum of 32 bins, and the populations of the bins are then used as the weighting factors g_i in eq A1. The bin sizes are chosen to be as small as possible and still include at least 95% of the total available vibrational energy. In addition, they are chosen to maintain an *average* vibrational energy within 0.01 eV of the average of the model frequencies used, which is calculated exactly in order to make the comparison. The bin sizes tend to be about 100–400 cm^{-1}, that is, about the same as the experimental uncertainty in the energy scale, 150–250 cm^{-1} (CM) for these systems.

CID thresholds are determined by using eq A1 and the vibrational energies listed in Table IV. The exact vibrational frequencies are not known for the $Fe(CO)_x^+$ ions. We therefore chose to approximate the vibrational distribution of states in a number of different ways to see what effect various assumptions about the vibrational frequency distribution have on the model thresholds. For $Fe(CO)_5^+$, we used the known frequencies for neutral $Fe(CO)_5$.[3] For $Fe(CO)_5$, the C–O stretching frequencies are all about 2000 cm^{-1}, the C–Fe–C bends are about 100 cm^{-1}, and the Fe–C stretches and Fe–C–O bends are about 400–600 cm^{-1}, so for each ion studied here, we used several model sets of frequencies covering these ranges. Frequencies were chosen to represent reasonable limits on the amount of vibrational energy that might be available, for example, making all of the Fe–C stretches 400 cm^{-1} in one model and all 600 cm^{-1} in another. A recent theoretical calculation[11] has predicted lower frequencies (e.g., ca 50 cm^{-1} for the C–M–C bend and 200 cm^{-1} for the M–C stretches), however, for $M(CO)_2^+$, with M = Sc, Cr, and Cu. It is plausible that the smaller $Fe(CO)_x^+$ ions similarly may also have lower frequencies, since they have less steric crowding. For the $Fe(CO)_x^+$ ions (x = 2–3), we therefore also used models in which the vibrational frequencies were similar to those of the calculation. We find that, in general, the measured CID threshold is fairly insensitive to the particular assumptions made about the exact vibrational frequencies, typically varying by less than 5%. The uncertainties in the results listed in Table III include the spread in values obtained when different model vibrational parameters were used for the same data set in addition to the other sources of uncertainty listed above.

It is also possible that rotational energy can couple into the reaction coordinate. For linear ions, this means that as much as k_BT (0.026 eV at 300 K) energy may be available for promoting reaction, and for nonlinear polyatomic ions, the amount of availabie energy is $3k_BT/2$. Because the rotational energy distribution should be more strongly peaked than the vibrational energy distribution, we simply add this amount to the measured thresholds to account for it.

(66) Sunderlin, L. S.; Armentrout, P. B. *J. Phys. Chem.* **1988**, *92*, 1209.
(67) Beyer, T.; Swinehart, D. F. *Commun. ACM* **1973**, *16*, 379. Stein, S. E.; Rabinovitch, B. S. *J. Chem. Phys.* **1973**, *58*, 2438, *Chem. Phys. Lett.* **1977**, *49*, 183. Gilbert, R. G.; Smith, S. C. *Theory of Unimolecular and Recombination Reactions*; Blackwell Scientific Publications: Oxford, 1990.